KSCE Journal of Civil Engineering (2022) 26(6):2877-2887
DOI 10.1007/s12205-022-1906-3

pISSN 1226-7988, eISSN 1976-3808
www.springer.com/12205

Structural Engineering

Study on Partial Factors and Combination Value Coefficients for Uniform Temperature Action of Large-Span Structures

Yuqing Yang[a], **Zaigen Mu**[a], **Yuxuan Wu**[a], **and Zhong Fan**[b]

[a]*School of Civil and Resource Engineering, University of Science and Technology Beijing, Beijing 100083, China*
[b]*China Architecture Design & Research Group, Beijing 100044, China*

ARTICLE HISTORY

Received 20 October 2021
Revised 19 January 2022
Accepted 2 February 2022
Published Online 1 April 2022

KEYWORDS

Thermal action
Closure temperature
Partial factor
Combination value coefficient
Reliability

ABSTRACT

The closure temperature refers to the temperature at which a structure forms an overall constrained structural system, also called the initial temperature. A reasonable closure temperature can avoid large additional stresses caused by excessive air temperature changes in large-span structures. To study the thermal action of the closure temperature on a structure, a probability distribution function of uniform temperature action is proposed. The effect of closure temperature is studied by introducing an adjustment coefficient. The partial factor and combination value coefficient of thermal action are presented, and their reliabilities are verified by the first-order second-moment method. The results show that with increasing adjustment coefficient, the probability distribution of thermal action tends to be uniformly divergent, the partial factor of thermal action increases, and the combination value coefficient decreases. The optimal closure temperature times are in March, April, October, and November for six cities in China. In this case, an adjustment coefficient of 0.3, a partial factor of 1.5, and the combination value coefficient of 0.45 are recommended. In addition, the partial factor of 1.5 and the combination value coefficient of 0.45 can be verified by reliability verification, which is more economical and reasonable with regard to ensuring safety.

1. Introduction

Thermal action is a variable load. Air temperature changes cause deformations of structural members, and temperature internal forces will be generated in the structure. For example, in bridge structures, air temperature changes and solar radiation have a significant effect on the internal forces (Wang et al., 2020); thus, thermal action needs to be considered in the design of bridge structural loads. In the analysis of large-span structures, such as stadiums and airport terminals, the effect of thermal action has attracted the attention of engineers and researchers.

The closure temperature refers to the temperature at which the large-span structure is closing or healing to form an overall constrained structural system. It is one of the important influencing factors on the air temperature effect of structures (Fan et al., 2007; Liu et al., 2020). The closure temperature, also known as the initial temperature, is usually taken as an interval near the annual average temperature. In this way, the closure temperature is in the middle of the highest and lowest temperatures, and the stress changes caused by thermal action are more uniform.

Scholars have conducted much research on the effect of air temperature, and the effect of thermal action on the stress and displacement of supertall and large-span structures cannot be ignored (Gao et al., 2019; Hu et al., 2020). Liu et al. (2012, 2015) found that solar radiation has a significant effect on the temperature stress distribution of steel members. The negative temperature difference affects the stress of the members, and the positive temperature difference affects the displacement. Chen et al. (2017, 2018, 2020) investigated the relationship between the nonuniform air temperature distribution and the thermal stress of steel structures through experiments and finite element simulations and proposed a simplified calculation method based on steady state analysis within an error of 5%. Fan et al. (2007, 2013) proposed that large-span steel structures need to consider the closure temperature. To meet the phased construction requirements of large-span structures, the closure temperature of each block is determined according to the construction plan and implementation status by analysing the weather and temperature change pattern of the proposed site over the years.

CORRESPONDENCE Yuqing Yang ✉ yqyang@ustb.edu.cn School of Civil and Resource Engineering, University of Science and Technology Beijing, Beijing 100083, China

Reliability analysis is necessary to determine the partial factors and combination value coefficients of thermal action. When a coefficient passes the reliability analysis, this coefficient can ensure safety and meet the code requirements of the specification. In terms of the reliability of structures, the first-order second-moment method (FOSM), Monte-Carlo method, and response surface method are the main calculation methods (Cornell, 1969; Rajashekhar and Ellingwood, 1993). Smedt et al. (2020) investigated the effect of reliability on the membrane structure by using the first-order reliability method and calibrated the partial factors. Tian et al. (2021) introduced the concept of the peak wind pressure coefficient, which can determine the roof load more reasonably. Gong and Wei (2007) and Gong and Zhao (2001) studied the reliability index calculation method of random variables that do not follow the normal distribution case, and gave the analytical solution of the probability distribution function for two load combinations in the design reference period.

Currently, a reasonable interval value for the closure temperature is not clear, and there have been few studies on partial factors and combination value coefficients of thermal action in existing codes or papers. Therefore, this paper analyses the temperature changes based on the air temperature data of representative cities in China and proposes a reasonable adjustment coefficient to determine the interval value of the closure temperature. In addition, the partial factors and the combination value coefficients of thermal action are also presented, and their reliability is verified. The values of partial factors and combination value coefficients are suggested for reference to similar projects.

2. Methods

By introducing an adjustment coefficient, the upper and lower limits of the closure temperature are defined. The distribution function of the closure temperature and the cumulative distribution function (CDF) of the uniform temperature action are given. In addition, according to the calculation method of partial factors and combination value coefficients, the formulas for partial factors and combination value coefficients of the uniform temperature action are derived.

2.1 Closure Temperature

The reference air temperature T is the reference value for air temperature and is the primary meteorological parameter required to determine the thermal action. The reference air temperature T includes monthly average maximum temperature $T_{m,max}$ and monthly average minimum temperature $T_{m,min}$ with a 50 year return period, which shall be statistically determined according to the average value of the maximum temperature in the month with the highest temperature over the years and the average value of the minimum temperature in the month with the lowest temperature (GB 50009-2012, 2012). The Load Code for the Design of Building Structure (GB 50009-2012, 2012) assumed that the reference air temperature T follows the Type I (Gumbel) extreme value distribution. The CDF and probability density function (PDF) of reference air temperature T can be derived from Eqs. (1) and (2), respectively (Kotz and Nadarajah, 2000). The mean value μ and the standard deviation σ of the temperature distribution can be determined by Eqs. (3) and (4), respectively:

$$F(T)=e^{-e^{-\alpha(T-u)}}, \tag{1}$$

$$f(T)=\alpha e^{-e^{-\alpha(T-u)}}e^{-\alpha(T-u)}, \tag{2}$$

$$\mu=u+\frac{0.5772}{\alpha}, \tag{3}$$

$$\sigma=\frac{\pi}{\sqrt{6}\alpha}, \tag{4}$$

where u is the location parameter and α is the scale parameter.

The maximum temperature difference ΔT_{max} is a constant calculated from temperature data according to Eq. (5):

$$\Delta T_{max}=T_{m,max}-T_{m,min}. \tag{5}$$

Generally, the value of closure temperature T_0 is close to a range of the average temperature $\overline{T}$, but this range is not uniform and clear. In this paper, an adjustment factor λ_T is introduced to define the value interval of the closure temperature. The maximum $T_{0,max}$ and the minimum $T_{0,min}$ limit values for the closure temperature T_0 are defined as follows:

$$T_{0,max}=\overline{T}+\lambda_T\Delta T_{max}/2\left(\lambda_T=0,0.1,0.2,...,0.5\right), \tag{6}$$

$$T_{0,min}=\overline{T}-\lambda_T\Delta T_{max}/2(\lambda_T=0,0.1,0.2,\ldots,0.5). \tag{7}$$

By changing the adjustment factor λ_T to change the value range of the closure temperature. When $\lambda_T=0$, the upper and lower limits of the closure temperature are the same, and they are equal to the average temperature $T_0=\overline{T}$. When $\lambda_T=0.5$, the upper and lower limits of the closure temperature include more than half of the temperature values of a year. When $\lambda_T>0.5$, the difference between positive (T+) and negative (T-) temperatures is too large, which is not considered reasonable in engineering projects and is not recommended at this stage. Therefore, in this paper, the adjustment coefficient λ_T is considered to be between 0 and 0.5.

2.2 Probability Distribution Function of Uniform Temperature Action

The closure temperature T_0 fluctuates between the maximum closure temperature $T_{0,max}$ and the minimum closure temperature $T_{0,min}$. Because the closing time is artificially determined within an appropriate temperature and time with actual engineering and personal experience, the closure temperature can be assumed to follow a uniform distribution. Thus, the distribution function of the closure temperature is assumed to be Eq. (8):

$$F_{T_0}(T_0)=\begin{cases}0 & T_0<T_{0,min}\\ \dfrac{T_0-T_{0,min}}{T_{0,max}-T_{0,min}} & T_{0,min}\le T_0\le T_{0,max}\\ 1 & T_0>T_{0,max}.\end{cases} \tag{8}$$

The uniform temperature action on the structure needs to consider two working conditions: temperature rise and temperature fall (GB 50009-2012, 2012), i.e., the effect of temperature difference. When the closure temperature is used as the initial temperature, the positive ΔT^+ and negative ΔT^- temperature differences are defined as Eq. (9):

$$\begin{cases}\Delta T^+ = T_{\max} - T_0 \\ \Delta T^- = T_{\min} - T_0 .\end{cases} \tag{9}$$

In summary, this paper assumes that the reference air temperature T follows the Gumbel distribution and that the closure temperature T_0 follows the uniform distribution. The closure temperature T_0 is defined based on the average temperature $\overline{T}$, while the reference air temperature T is calculated based on the measured temperature data. The correlation between T and T_0 is very small, thus these two random variables are considered to be independent of each other. Therefore, the CDF of the uniform temperature action is given as Eq. (10), and the PDF of the uniform temperature action is given as Eq. (11):

$$\begin{aligned} F_{\Delta T}(\Delta T) &= P(T - T_0 \le \Delta T) = \iint_{T-T_0 \le \Delta T} f_T(T) f_{T_0}(T_0)\, \mathrm{d}T \mathrm{d}T_0 \\ &= \int_{T_{0,\min}}^{T_{0,\max}} \frac{1}{T_{0,\max} - T_{0,\min}} F_T(\Delta T + T_0)\, \mathrm{d}T_0 \\ &= \frac{1}{T_{0,\max} - T_{0,\min}} \int_{T_{0,\min}}^{T_{0,\max}} F_T(\Delta T + T_0)\, \mathrm{d}T_0 , \end{aligned} \tag{10}$$

$$f_{\Delta T}(\Delta T) = \frac{1}{T_{0,\max} - T_{0,\min}} \left[F_T(T_{0,\max} + \Delta T) - F_T(T_{0,\min} + \Delta T) \right] . \tag{11}$$

2.3 Partial Factor and Combination Value Coefficient

The partial factor is the ratio of the design value of the dominant variable action Q_{1d} to its standard value Q_{1k}. According to ES 1990-2002 (2002), the partial factor of the dominant variable action is defined as Eq. (12):

$$\gamma_{Q_1} = \frac{Q_{1d}}{Q_{1k}} = \frac{F_X^{-1}\left[\Phi\left(-\alpha_{Q_1}\beta_T\right)\right]}{Q_{1k}} , \tag{12}$$

where Q_{1d} denotes the design value of the dominant variable action, Q_{1k} denotes the standard value of dominant variable action, $F_X^{-1}(x)$ denotes the inverse function of the CDF of the dominant variable action, β_T is the target reliability index, and α_{Q_1} is the sensitivity factor of the dominant variable action, which is taken as -0.7 (ES 1990-2002, 2002; GB 50068-2018, 2018).

The partial factor for the accompanying variable action is defined as Eq. (13) (ES 1990-2002, 2002):

$$\gamma_{Q_i} = \frac{Q_{id}}{Q_{ik}} = \frac{F_{Q_i}^{-1}\left\{\left[\Phi\left(-\alpha_{Q_i}\beta_T\right)\right]^m\right\}}{Q_{ik}} , \tag{13}$$

where Q_{id} denotes the design value of the accompanying variable action, Q_{ik} denotes the standard value of the accompanying variable action, $F_{Q_i}^{-1}(x)$ denotes the inverse function of the CDF of the accompanying variable action, and α_{Q_i} is the sensitivity factor of accompanying variable action, which is taken as -0.28 (ES 1990-2002, 2002; GB 50068-2018, 2018).

The combination value coefficient is the ratio of the partial factor of accompanying variable action γ_{Q_i} to the partial factor of dominant variable action γ_{Q_1}, as shown in Eq. (14):

$$\varphi_T = \frac{\gamma_{Q_i}}{\gamma_{Q_1}} . \tag{14}$$

In Sections 2.1 – 2.2, the CDF of the uniform temperature action considering the closure temperature is derived, and by bringing them into Eqs. (12) – (14), the partial factors and combination value coefficients corresponding to the adjustment factor λ_T can be calculated. Specifically, when $\lambda_T = 0$, the uniform temperature action follows a Gumbel distribution, the design value of the accompanying variable action can be expressed as Eq. (15), and the design value of the dominant variable action can be expressed as Eq. (16). Because the various distribution functions follow the Gumbel distribution, u and α in Eqs. (15) and (16) is given as Eqs. (3) and (4), respectively. By taking Eqs. (15) and (16) into Eqs. (12) – (14), the partial factor can be expressed as Eq. (17), and the combination value coefficient can be expressed as Eq. (18) (Gong and Wei, 2007):

$$Q_{1d} = F_X^{-1}\left[\Phi\left(-\alpha_{Q_1}\beta_T\right)\right] = u - \frac{1}{\alpha}\ln\{-\ln\Phi(0.7\beta_T)\} , \tag{15}$$

$$Q_{id} = F_{Q_i}^{-1}\left\{\left[\Phi\left(-\alpha_{Q_i}\beta_T\right)\right]^m\right\} = u - \frac{1}{\alpha}\ln\{-\ln[\Phi(0.28\beta_T)]^m\} , \tag{16}$$

$$\gamma_T = K_T\left(1 - 0.779V_T\left\{0.577 + \ln\left[-\ln\Phi\left(0.7\beta_T\right)\right]\right\}\right) , \tag{17}$$

$$\varphi_T = \frac{\left(1 - 0.779V_T\left\{0.577 + \ln\left[-\ln\Phi\left(0.28\beta_T\right)^m\right]\right\}\right)}{\left(1 - 0.779V_T\left\{0.577 + \ln\left[-\ln\Phi\left(0.7\beta_T\right)\right]\right\}\right)} , \tag{18}$$

$$K_T = \mu_T / \Delta T_k , \tag{19}$$

$$V_T = \sigma_T / \mu_T , \tag{20}$$

where K_T is the mean coefficient of the uniform temperature action, V_T is the coefficient of variation of the uniform temperature action, ΔT_k is the characteristic value of the uniform temperature action, μ_T is the mean value, and σ_T is the standard deviation.

3. Temperature Data Analysis

Six cities (City A – City F) represent the temperature characteristics of six major regions in Northeast, North, Northwest, Southwest, Central, and South China, as shown in Table 1. Temperature data for the past 50 years (1970 – 2020) were collected from the National Climatic Data Center (NCDC, 2021), and the monthly

Table 1. Latitude, Altitude and Monthly Temperature of Six Cities

City	Latitude	Altitude/m	$T_{m,max}$/°C	$T_{m,min}$/°C	ΔT/°C
Harbin (City A)	45°56′	118.3	31.427	-30.200	61.627
Beijing (City B)	39°48′	31.3	34.513	-12.410	46.923
Lanzhou (City C)	36°30′	1517.2	33.439	-12.984	46.423
Shanghai (City D)	31°12′	4.6	36.845	-1.287	38.132
Chengdu (City E)	30°45′	547.7	33.374	-0.068	33.442
Guangzhou (City F)	23°13′	70.7	35.142	6.510	28.632

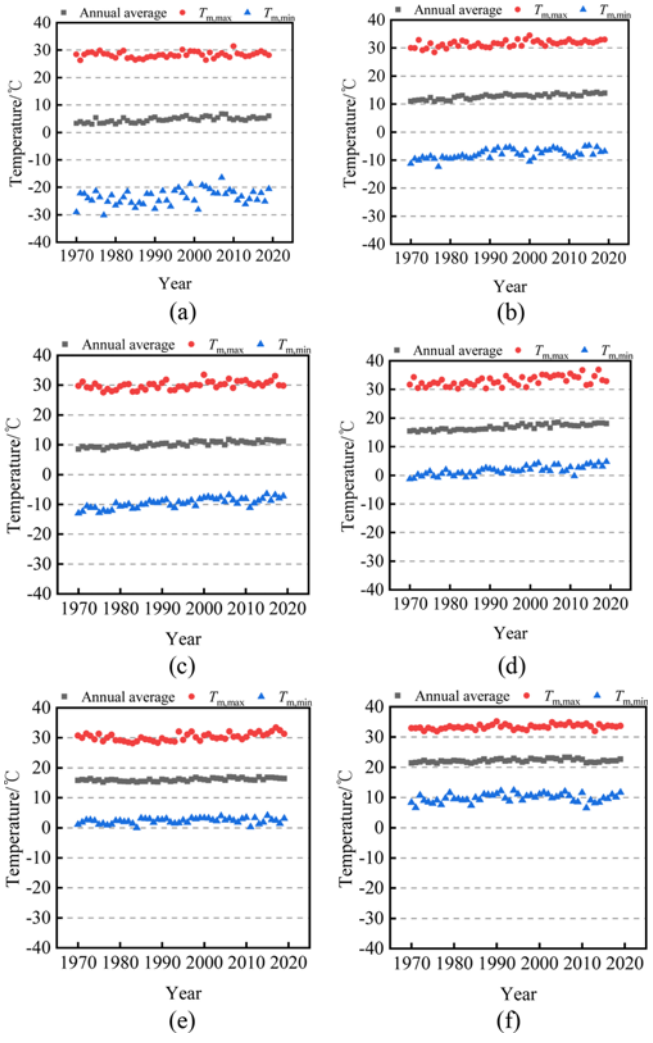

Fig. 1. Temperature Variation of Six Cities in the Past 50 Years: (a) City A, (b) City B, (c) City C, (d) City D, (e) City E, (f) City F

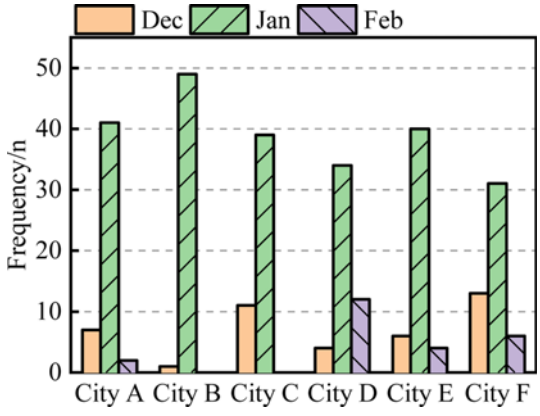

Fig. 2. Histogram of the Month of the Maximum Monthly Average Temperature

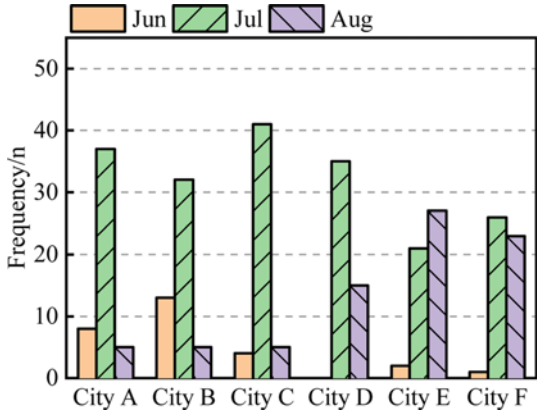

Fig. 3. Histogram of the Month of the Minimum Monthly Average Temperature

average temperatures were analysed to obtain statistics on the temperature changes in each city.

3.1 Monthly Average Temperature

The extreme monthly average temperatures and temperature differences ΔT of the six cities are shown in Table 1, and Fig. 1 presents the monthly average temperature over the past 50 years. The differences in the maximum monthly temperature are small, all fluctuating at approximately 30°C. Both the annual temperature and the minimum monthly temperature are related to latitude, and the minimum monthly temperature in the north is much lower than that in the south. The degree of dispersion between the annual temperature and the maximum monthly temperature is not large, and the minimum monthly temperature fluctuates greatly. In addition, the annual temperature and the extreme monthly temperature both show an overall increasing trend.

Statistics on the months of the extreme monthly average temperature are shown in Figs. 2 and 3. The months with maximum temperature are distributed in June, July, and August, mainly in July and August, and the moths with minimum temperature are distributed in January, February, and December, mainly in January.

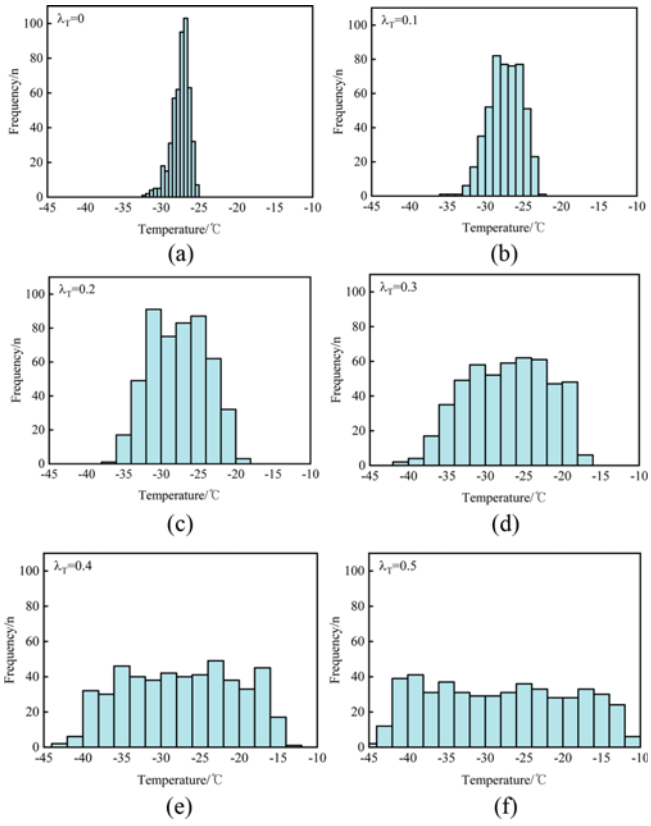

Fig. 4. Statistical Histogram of the Negative Temperature Difference in City B: (a) $\lambda_T = 0$, (b) $\lambda_T = 0.1$, (c) $\lambda_T = 0.2$, (d) $\lambda_T = 0.3$, (e) $\lambda_T = 0.4$, (f) $\lambda_T = 0.5$

3.2 Effect of Adjustment Coefficients on the Temperature Difference Distribution

The temperature data from Section 3 are brought into the calculation method in Section 2. Then the relationship between the adjustment coefficients of the six cities and the partial factors and the combination value coefficients are obtained, and their suggested values are given.

Taking City B as an example, the adjustment coefficients λ_T take the value of 0, 0.1, ..., 0.4, 0.5. According to Eqs. (10) and (12) – (14), the statistical histogram of the negative temperature difference ΔT^- in City B is calculated in Fig. 4. When $\lambda_T = 0$, the uniform temperature action follows the Gumbel distribution in Fig. 4(a). As the adjustment coefficient increases, the distribution of the temperature difference effect is gradually dispersed. The amount of data between the bins becomes closer to the average, and the distribution is increasingly different from the Type I (Gumbel) extreme value distribution.

3.3 Effect of Adjustment Coefficients on the Partial Factor and Combination Value Coefficient

According to Eqs. (17) and (18), the partial factor and combination value coefficient for the effect of positive and negative temperature differences in the six cities are obtained. The adjustment factor λ_T is refined to a value interval of 0.01 and the effect of the adjustment factor on the partial factors and combination value coefficients of the temperature difference effect is analysed. The relationship between the partial factor and combination value coefficient of the uniform temperature action and the adjustment coefficient is shown in Figs. 5 and 6, respectively. The partial factors of the six cities are positively correlated with the adjustment coefficients λ_T. The partial factors increase slowly in the initial stage ($0 < \lambda_T < 0.15$), and increase approximately linearly in the subsequent stage ($0.15 < \lambda_T < 0.5$). The combination value coefficients of the six cities are negatively correlated with the adjustment coefficient of closure temperature λ_T. The combination value coefficients increase slowly in the initial stage ($0 < \lambda_T < 0.05$) and increase approximately linearly in the subsequent stage. When the closure temperature is taken as the annual average temperature value, i.e., $\lambda_T = 0$, the partial factor is 1.25, and the combination value coefficient is 0.7. In this case, the partial factor is small, and the combination value coefficient is large.

The partial factors of positive and negative temperature differences in different cities are closer when they reach 1.5. At this time, the adjustment coefficients of the positive temperature difference range from 0.28 to 0.33, and the negative temperature difference is from 0.28 to 0.35. In general, when the adjustment

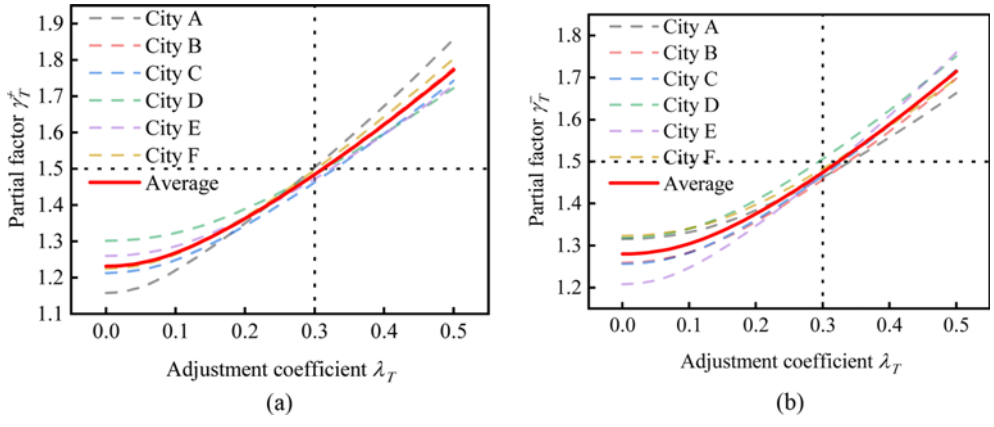

Fig. 5. Relationship between the Adjustment Coefficient and Partial Factor of Uniform Temperature Action: (a) Positive Temperature Difference, (b) Negative Temperature Difference

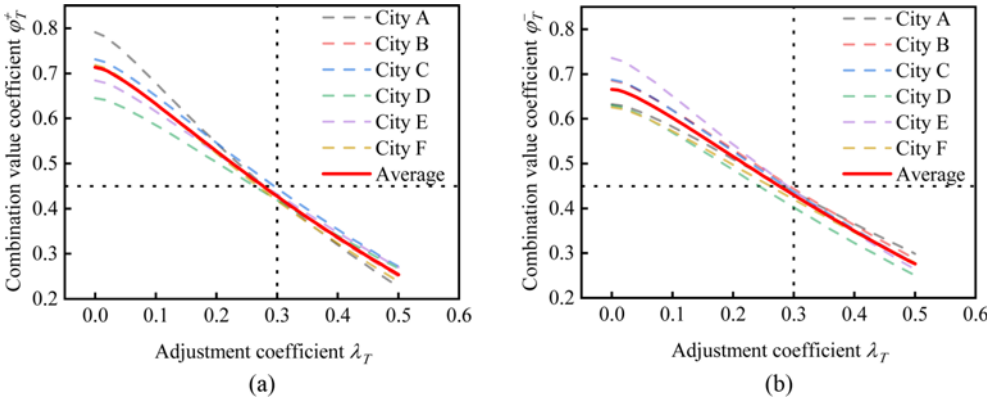

Fig. 6. Relationship between the Adjustment Coefficient and Combination Value Coefficient of Uniform Temperature Action: (a) Positive Temperature Difference, (b) Negative Temperature Difference

coefficient is 0.3, the partial factor is 1.50, and the combined value coefficient is 0.45. In this case, the partial factor is 1.5, which is the same as the partial factor in the Unified Standard for Reliability Design of Building Structures (GB 50068-2018, 2018).

4. Discussion

4.1 The Value of the Adjustment Coefficient

It is suggested that the positive and negative temperature differences of the structure are the same; however, the closure time of the project is uncertain. To facilitate engineering applications as much as possible, the partial factor and combination value coefficient of the uniform temperature action should be selected reasonably, and the closing time and adjustment coefficient are discussed as follows.

First, the different adjustment coefficients λ_T are chosen to calculate the upper and lower limits of the closure temperature ($T_{0,\max}$, $T_{0,\min}$), and these values are compared with the daily average temperature data $\overline{T}_d$. The number of days included in the upper and lower limits ($T_{0,\min} \le \overline{T}_d \le T_{0,\max}$) is checked and compared with the total number of days over 50 years to obtain the rate of included days. Taking City B as an example, the relationship between the adjustment coefficient and the number of included days is obtained (in Fig. 7). As shown in Fig. 7, when the adjustment coefficient λ_T is 0.3, approximately 30% of the days are included, which is in the range of optimal closing times and is consistent with engineering experiences. When the adjustment coefficient λ_T is 0.5, approximately 60% of the days are included, which makes the difference between positive (T+) and negative (T-) temperatures too large.

Next, the relationship between the adjustment coefficients λ_T and the monthly average temperature is analysed. The upper and lower limits of the closure temperature are calculated with different adjustment coefficients. The monthly average temperature of each month in City B is shown in Fig. 8. April and October are closest to the 50-year average temperature $\overline{T}$ in City B. When the adjustment coefficient is 0.3, the months roughly included are March, April, October, and November, which means that the range of the optimal closure time of the year is covered. The remaining five cities have geographical areas that are slightly different from City B, but the trend of the relationship between the closure time and the adjustment coefficient is the same. According to the closure time, existing codes, and safety of the project, it is recommended that the adjustment coefficient of closure temperature λ_T is 0.3, the partial factor is 1.5, and the combination value coefficient is 0.45. Moreover, it is recommended

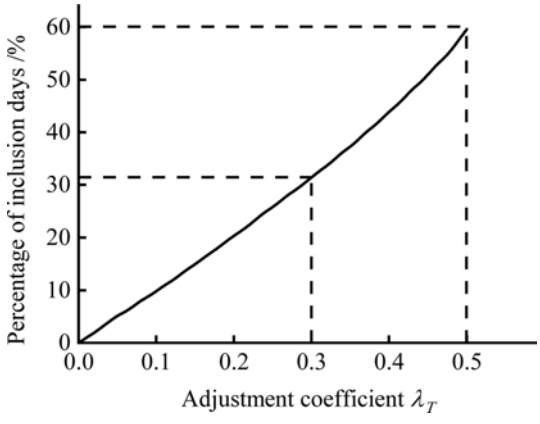

Fig. 7. Relationship between the Adjustment Coefficient and Percentage of Inclusion Days

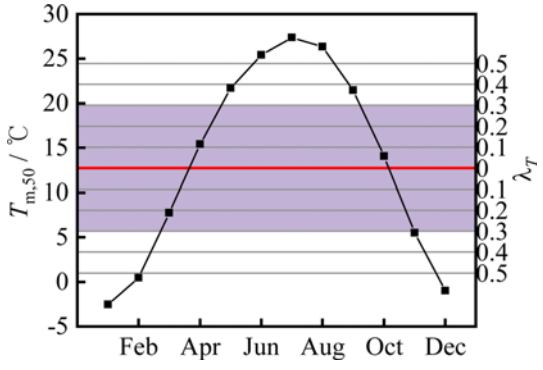

Fig. 8. Monthly Average Temperature of City B in 50 Years

the actual project closes in March, April, October, and November.

4.2 Reliability Analysis of the Partial Factor

In the reliability analysis of the partial factor, only the combination case of permanent action and temperature action is considered, and the structural ultimate limit state equation is determined as Eq. (21):

$$Z = g(X_1, X_2, ..., X_n) = R - S_G - S_T = 0 \,, \tag{21}$$

where $X_i (i = 0, 1, \ldots, n)$ denotes a random variable; R is the random variable of the structural resistance, which follows the log-normal distribution; S_G is the random variable of permanent action, which follows the normal distribution, with statistical parameters $k_{S_G} = \frac{\mu_{S_G}}{S_{Gk}} = 1.06$ and $\delta_{S_G} = \frac{\sigma_{S_G}}{\mu_{S_G}} = 0.07$; and S_T is the random variable of the temperature action. The probability distribution function is given by Eq. (10).

The reliability index of the structural elements should be calculated iteratively according to the following formula (GB 50009-2012, 2012):

$$\beta = \frac{\mu_{Z'}}{\sigma_{Z'}} = \frac{g_X(x_1^*, x_2^*, ..., x_n^*) + \sum_{i=1}^{n} \left.\frac{\partial g_X}{\partial X_i}\right|_P \left(\mu_{X_i'} - x_i^*\right)}{\left(\sum_{i=1}^{n} \left(\left.\frac{\partial g_X}{\partial X_i}\right|_P \sigma_{x_i'}\right)^2\right)^{\frac{1}{2}}} \,. \tag{22}$$

The positive temperature action of reinforced concrete structural members in six cities is analysed for four stress states (axial tension, axial compression, bending, and shear). The effect ratio ρ of temperature action to permanent load is taken as $\rho = S_{Tk}/S_{Gk}$. Based on actual engineering experience, the effect ratio ρ is between 0.1 and 0.5, i.e., ρ is taken as $\rho = 0.1, 0.2 \ldots, 0.5$. The FOSM is used to calculate the reliable index β of the partial factor of uniform temperature action.

From Fig. 9, with increasing of the effect ratio ρ, the reliability indexes β show a trend of first increasing and then decreasing. For the two states of axial tension and bending, the steel bars play a major role, and the target reliability index β_T is 3.2. The turning point of the reliability index curve is approximately 0.2. For the other two states of axial compression and shear, concrete plays a major role, and the target reliability index β_T is 3.7. The turning point of the reliability index curve is approximately 0.3. With increasing effect ratio ρ, the reliability index curves of each city are gradually separated. Because the temperature difference varies in each city, the larger the effect ratio ρ is, the greater the proportion of the temperature difference in the load combination. Therefore, the reliability index β of each city gradually increases with the increasing of effect ratio ρ.

4.3 Reliability Analysis of the Combination Value Coefficient

In the reliability analysis of the combination value coefficient,

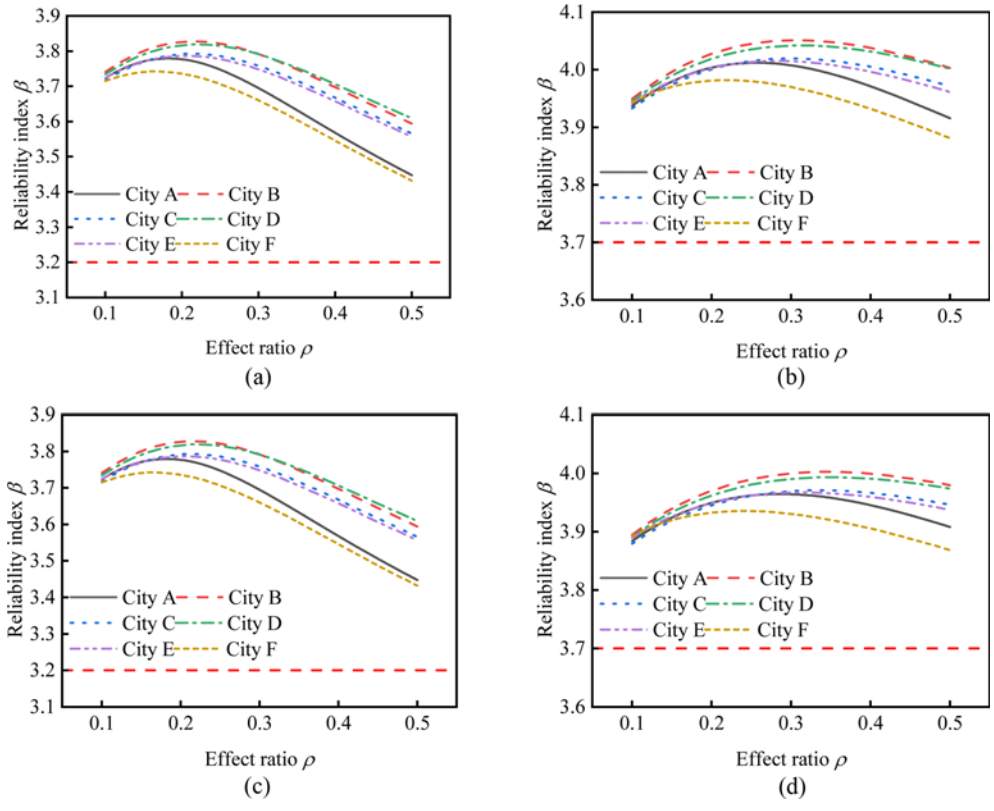

Fig. 9. Relationship between the Effect Ratio and Reliability Index of Reinforced Concrete Members: (a) Axial Tension, (b) Axial Compress, (c) Bending, (d) Shear

the permanent action, floor live load action, and temperature action are considered. The structural limit state equation is as follows:

$$Z = R - S_G - S_Q - S_T = 0 \ , \tag{23}$$

where S_Q is the random variable of floor live load action.

Two effect ratios $\rho_1 = S_{Qk} / S_{Gk}$ and $\rho_2 = S_{Tk} / S_{Gk}$ were set based on actual engineering experience. ρ_1 fluctuates between 0.2 and 1.0, and ρ_2 fluctuates between 0.1 and 0.5, spacing 0.1, i.e., ρ_1 = 0.2, 0.3, ..., 1.0 and ρ_2 = 0.1, 0.2, ..., 0.5. The FOSM is used to calculate the reliability index of the combination value coefficient. In addition, the reliability indexes of the combination value coefficients of 0.45 and 0.6 were compared. A combination value coefficient of 0.45 is the recommended value given in this paper, while a combination value coefficient of 0.6 is the value given in the Load Code for The Design of Building Structure (GB 50009-2012, 2012) which is based on design experience.

The target reliability indexes for the axial tension and bending states of reinforced concrete structural members are β_T = 3.2, and the target reliability indexes for the axial compression and shear states are β_T = 3.7. Taking axial tension and axial compression as examples, the reliability index of the positive temperature difference was calculated, as shown in Figs. 10 and 11, respectively. From Fig. 10, the average reliability index for the combination value coefficient of 0.45 is 4.146, which satisfies the target reliability index β_T = 3.2. In addition, the reliability index for the combination value coefficient of 0.6 is 4.328, which meets the requirement but is much higher. In comparison, the combination value coefficient of 0.45 is more economical and reasonable than that of 0.6. From Fig. 11, the average reliability index for the combination value coefficient of 0.45 is 4.414, and that of 0.6 is 4.553. Both of them meet the requirement but the combination value coefficient of 0.45 is more suitable for adoption.

5. Analysis of Engineering Applications

The above research results are applied to an airport project for temperature effect analysis. To determine whether the partial factor and the combination value factor meet the engineering requirements, the stress of the first floor slab under the most unfavourable combination in the nonseismic combination is determined.

5.1 Engineering Background

The T1 terminal of Xiamen Xiang'an International Airport (Fig. 12) has a total construction area of approximately 660,000 square metre and consists of two parts: the main building and the finger corridor. The main building includes one underground floor and three aboveground floors, and it is approximately 468 m in length and 354 m in width. The majority of buildings are reinforced

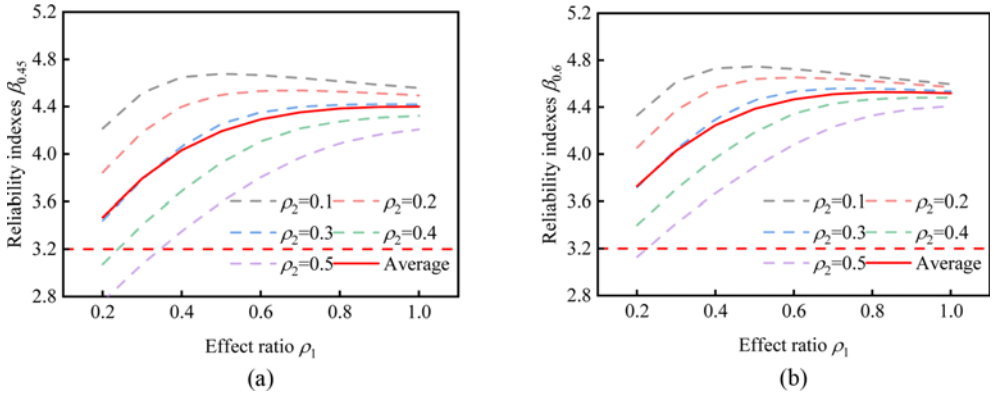

Fig. 10. Reliability Indexes of Reinforced Concrete Structures with Axial Tension: (a) Axial Tension of 0.45, (b) Axial Tension of 0.6

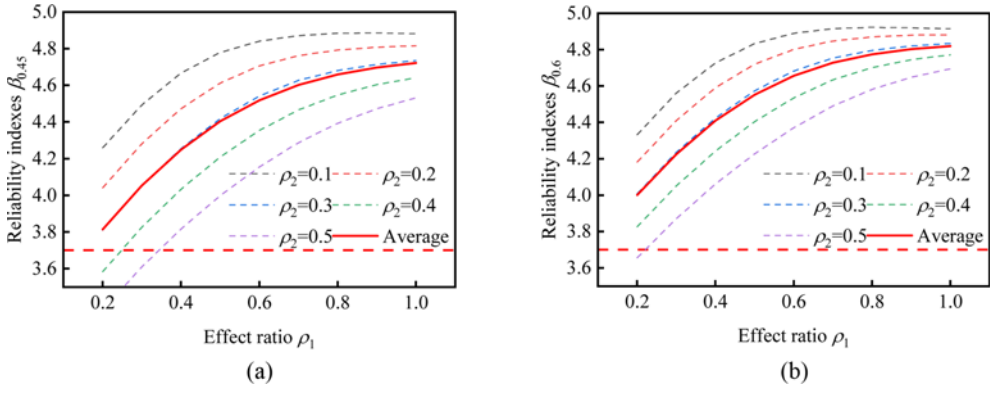

Fig. 11. Reliability Indexes of Reinforced Concrete Structures with Axial Compression: (a) Axial Compression of 0.45, (b) Axial Compression of 0.6

Fig. 12. T1 Terminal of the Xiang'an Airport

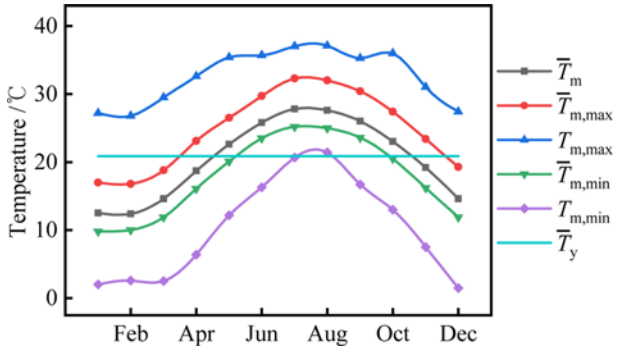

Fig. 13. Characteristics of Xiamen Temperature

Table 2. Nonseismic Load Combinations

Num	Load combinations	Num	Load combinations
1-1	1.0DL	6-1	1.3DL+1.5LL+0.45×1.5PTD
2-1	1.0LL	6-2	1.3DL+1.5LL+0.45×1.5NTD
3-1	1.0DL+1.0LL	6-3	1.0DL+1.5LL+0.45×1.5PTD
4-1	1.3DL+1.5LL	6-4	1.0DL+1.5LL+0.45×15NTD
4-2	1.0DL+1.5LL	7-1	1.3DL+0.7×1.5LL+1.5PTD
5-1	1.3DL+1.5PTD	7-2	1.3DL+0.7×1.5LL+1.5NTD
5-2	1.3DL+ 1.5NTD	7-3	1.0DL+0.7×1.5LL+1.5PTD
5-3	1.0DL+1.5PTD	7-4	1.0DL+0.7×1.5LL+1.5NTD
5-4	1.0DL+1.5NTD		

concrete frame structures with large-span steel structure roofs. This large-span structure is a structure that combines reinforced concrete and steel structures and should be analysed for temperature difference action because of the complicated construction and irregular structure shape. The temperature change in Xiamen is shown in Fig. 13.

5.2 Load Combination

The load conditions for the nonseismic combinations are shown in Table 2. In nonseismic combination cases, a partial factor of 1.5 and a combination value coefficient of 0.45 are used to combine the dead load (DL), live load (LL), and temperature differences (TD). Temperature differences include positive temperature differences (PTDs) and negative temperature differences (NTDs).

5.3 Temperature Stress Analysis

According to the load combination of Table 2, the stresses of the first floor slab are calculated by SAP2000, and the most unfavourable cases are analysed. The combination of the most unfavourable cases is No.5-1 (1.3 DL + 1.5 PTD) and No.5-2 (1.3 DL + 1.5 NPD). Fig. 14 presents the stresses of the first floor slab for these two cases.

From Fig. 14, most of the stresses in the first floor slab under the combination of No.5-1 are tensile stresses, and some compressive stresses exist in the edge parts. Most of the X-directional stress in the middle part of the slab is 4 MPa, and the tensile stress gradually decreases to the left and right edges. Most of the Y-directional stress in the middle part of the slab is 3 MPa, and the tensile stress gradually decreases to the top and bottom edges. In the No.5-2 case, the stress in the first floor slab is compressive stress. Among them, the X-directional stress in the middle part of the slab reaches 7 MPa. The Y-directional stress in the middle part of the slab is approximately 6 MPa, and tensile stress exists at the top and bottom.

The tensile strength of C40 concrete is f_{tk} = 2.39 MPa; therefore, the temperature stress of the first floor slab is larger at present, and the temperature reinforcement measures of these two floors should be strengthened. The overall requirements are met, and local reinforcement measures should be taken.

6. Conclusions

1. The temperature data of representative cities are analysed. With decreasing latitude in the region, the temperature in the areas with high latitude gradually approaches the middle from a bimodal distribution and farther apart, and the interval between the two peaks gradually converges. The maximum monthly average temperature does not vary much from place to place, and the annual average temperature and minimum monthly average temperature are related to latitude and altitude.
2. A probability model of air temperature action considering the closure temperature distribution is established and compared

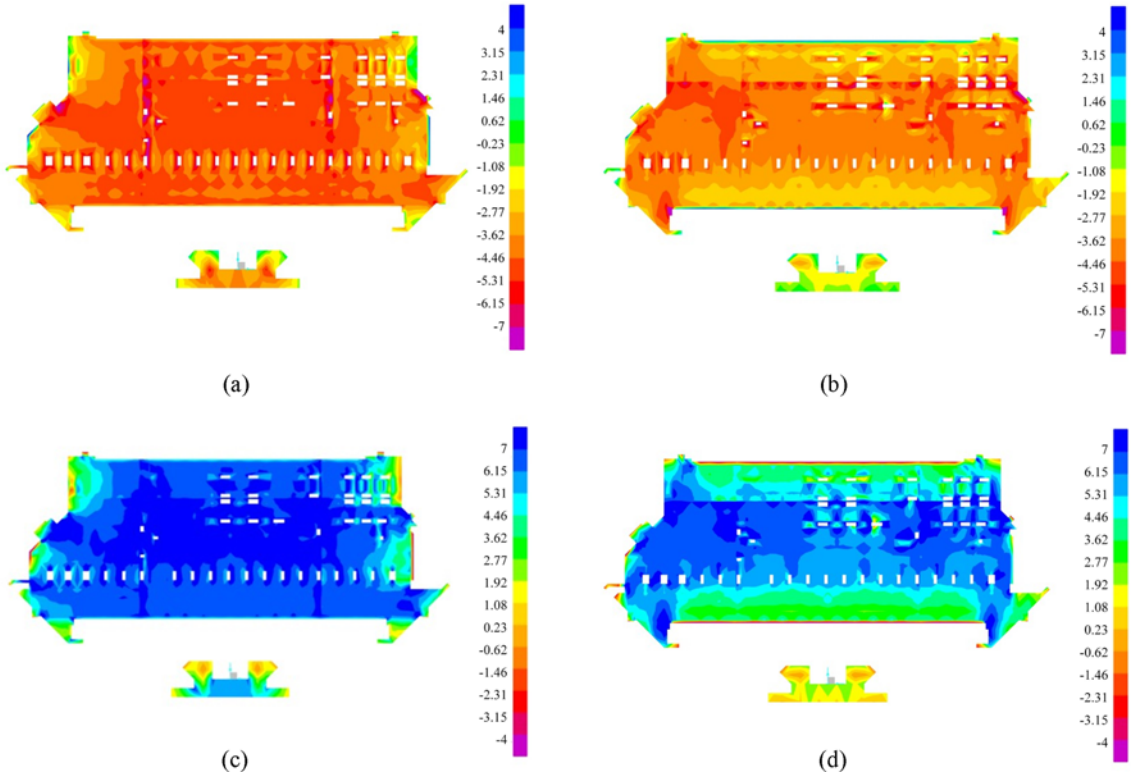

Fig. 14. Stress in the First Floor of the Most Unfavourable Combination (MPa): (a) X-Directional Stress of No.5-1, (b) Y-Directional Stress of No.5-1, (c) X-Directional Stress of No.5-2, (d) Y-Directional Stress of No.5-2

with the probability distribution of air temperature action considering only the average temperature value. Considering the closure temperature distribution, the partial factor and the combination value coefficient of the uniform temperature action are analysed. When the adjustment coefficient takes λ_T = 0.3, the partial factor is 1.5 and the combination value coefficient is 0.45. At this time, the closure time is within the optimal closure temperature range, and the actual project is suitable for closure in March, April, October, and November.

3. Different stress states of reinforced concrete members are selected, and the reliability indexes are verified for the partial factor and combination value coefficient. The results show that the reliability indexes of positive and negative temperature differences in the six cities are less different, although the geographical area and latitude are different, and the reliability indexes of each member under the force condition meet the target reliability index requirements. The reliability index of the combination value coefficient of 0.45 is smaller than that of 0.6, but the selection of 0.45 can reduce the energy and resource consumption appropriately.
4. The temperature stresses in the first floor slab of an airport terminal structure are analysed by applying the partial factor and combination value coefficient. In the nonseismic combination, the partial factor and combination value coefficient meet the safety requirements. The temperature stresses are approximately 3 – 7 MPa, and these results could serve as a reference for the project.

Acknowledgments

This work was supported by the National Natural Science Foundation of China (grant No. 51578064) and the Natural Science Foundation of Beijing (grant No.8172031).

ORCID

Yuqing Yang https://orcid.org/0000-0002-3152-5139

References

Chen DS, Qian HL, Wang HJ, Chen Y, Fan F, Shen SZ (2018) Experimental and numerical investigation on the non-uniform temperature distribution of thin-walled steel members under solar radiation. *Thin-Walled Structures* 122:242-251, DOI: 10.1016/j.tws.2017.10.018

Chen DS, Wang HJ, Qian HL, Li X, Fan F, Shen SZ (2017) Experimental and numerical investigation of temperature effects on steel members due to solar radiation. *Applied Thermal Engineering* 127:696-704, DOI: 10.1016/j.applthermaleng.2017.08.045

Chen DS, Xu WC, Qian HL, Sun JY, Li JF (2020) Effects of non-uniform temperature on closure construction of spatial truss structure. *Journal of Building Engineering* 32:101532, DOI: 10.1016/j.jobe.2020.101532

Cornell CA (1969) A probability-based structural code. *Journal of the American Concrete Institute* 66(12):974-985

ES 1990-2002 (2002) Basis of structural design. ES 1990-2002, British Standards Institution

Fan Z, Wang Z, Tang J (2007) Analysis on temperature field and

determination of temperature upon healing of large-span steel structure of the National Stadium. *Journal of Building Structure* 28(2):32-40, DOI: 10.14006/j.jzjgxb.2007.02.004 (in Chinese)

Fan Z, Zhao CJ, Zhang Y, Peng Y, Li JX, Yang JM (2013) Simulation technology for staged construction of large steel structure engineering. *Spatial Structure* 19(1):28-40, DOI: 10.13849/j.issn.1006-6578.2013.01.007 (in Chinese)

Gao F, Chen P, Xia Y, Zhu HP, Weng S (2019) Efficient calculation and monitoring of temperature actions on supertall structures. *Engineering Structures* 193:1-11, DOI: 10.1016/j.engstruct.2019.05.026

GB 50009-2012 (2012) Load code for the design of building structure. GB 50009-2012, China Construction Industry Press, Beijing, China

GB 50068-2018 (2018) Unified standard for reliability design of building structures. GB 50068-2018, China Construction Industry Press, Beijing, China

Gong JX, Wei WW (2007) Reliability design principle of engineering structure. China Machine Press, Beijing, China

Gong JX, Zhao GF (2001) Closed-form solution and simplification of combination of sustained load and transient load. *Engineering Mechanics* 18(6):11-17 (in Chinese)

Hu JH, Chen WJ, Ren SJ, Zhang SH, Qu YG, Yin Y, Yang DQ (2020) Building performance monitoring and analysis of a large-span aerogel-membrane airport terminal. *Engineering Structures* 219:110837, DOI: 10.1016/j.engstruct. 2020.110837

Kotz S, Nadarajah S (2000) Extreme value distributions: Theory and applications. Imperial College Press, London, UK

Liu HB, Chen ZH, Zhou T (2012) Theoretical and experimental study on the temperature distribution of H-shaped steel members under solar radiation. *Applied Thermal Engineering* 37:329-335, DOI: 10.1016/j.applthermaleng.2011.11.045

Liu HB, Liao XW, Chen ZH, Zhang Q (2015) Thermal behavior of spatial structures under solar irradiation. *Applied Thermal Engineering* 87:328-335, DOI: 10.1016/j.applthermaleng.2015.04.079

Liu J, Liu Y J, Zhang CY, Zhao QH, Lyu Y, Jiang L (2020) Temperature action and effect of concrete-filled steel tubular bridges: A review. *Journal of Traffic and Transportation Engineering (English Edition)* 7(2):174-191, DOI: 10.1016/j.jtte.2020.03.001

NCDC (2021) National Climatic Data Center, National Oceanic and Atmospheric Administration (NOAA), Retrieved June 1, 2021, https://www.ncei.noaa.gov/

Rajashekhar MR, Ellingwood BR (1993) A new look at the response surface approach for reliability analysis. *Structural Safety* 12(3):205-220, DOI: 10.1016/0167-4730(93)90003-J

Smedt ED, Mollaert M, Caspeele R, Botte W, Pyl L (2020) Reliability-based calibration of partial factors for the design of membrane structures. *Engineering Structures* 214:110632, DOI: 10.1016/j.engstruct.2020.110632

Tian YJ, Guan HW, Shao S, Yang QS (2021) Provisions and comparison of Chinese wind load standard for roof components and cladding. *Structures*, 33:2587-2598, DOI: 10.1016/j.istruc.2021.06.011

Wang ZW, Zhang WM, Tian GM, Liu Z (2020) Joint values determination of wind and temperature actions on long-span bridges: Copula-based analysis using long-term meteorological data. *Engineering Structures* 219:110866, DOI: 10.1016/j.engstruct.2020.110866